ORIGINAL ARTICLE

[18F]Flutemetamol amyloid-beta PET imaging compared with [11C]PIB across the spectrum of Alzheimer's disease

Shizuo Hatashita · Hidetomo Yamasaki · Yutaka Suzuki · Kumiko Tanaka · Daichi Wakebe · Hideki Hayakawa

Abstract

Purpose The aim was to identify the amyloid beta (Aβ) deposition by positron emission tomography (PET) imaging with the 18F-labeled Pittsburgh compound B (PIB) derivative [18F]flutemetamol (FMM) across a spectrum of Alzheimer's disease (AD) and to compare Aβ deposition between [18F]FMM and [11C]PIB PET imaging.

Methods The study included 36 patients with AD, 68 subjects with mild cognitive impairment (MCI), 41 older healthy controls (HC) (aged ≥56), 11 young HC (aged ≤45), and 10 transitional HC (aged 46–55). All 166 subjects underwent 30-min static [18F]FMM PET 85 min after injection, 60-min dynamic [11C]PIB PET, and cognitive testing. [18F]FMM scans were assessed visually, and standardized uptake value ratios (SUVR) were defined quantitatively in regions of interest identified on coregistered MRI (cerebellar cortex as a reference region). The PIB distribution volume ratios (DVR) were determined in the same regions.

Results Of 36 AD patients, 35 had positive scans, while 36 of 41 older HC subjects had negative scans. [18F]FMM scans had a sensitivity of 97.2 % and specificity of 85.3 % in distinguishing AD patients from older HC subjects, and a specificity of 100 % for young and transitional HC subjects. The [11C]PIB scan had the same results. Interreader agreement was excellent (kappa score=0.81). The cortical FMM SUVR in AD patients was significantly greater than in older HC subjects (1.76±0.23 vs 1.30±0.26, $p < 0.01$). Of the MCI patients, 68 had a bimodal distribution of SUVR, and 29 of them (42.6 %) had positive scans. Cortical FMM SUVR values were strongly correlated with PIB DVR ($r = 0.94$, $n = 145$, $p < 0.001$).

Conclusion [18F]FMM PET imaging detects Aβ deposition in patients along the continuum from normal cognitive status to dementia of AD and discriminates AD patients from HC subjects, similar to [11C]PIB PET.

Keywords Alzheimer's disease · Amyloid imaging · PET · Amyloid beta (Aβ)

S. Hatashita (✉) · H. Yamasaki
Neurology, PET Center, Shonan-Atsugi Hospital, 118-1 Murumizu, Atsugi 243-8551, Japan
e-mail: shizu@olive.ocn.ne.jp

Y. Suzuki · D. Wakebe · H. Hayakawa
Radiology, PET Center, Shonan-Atsugi Hospital, Atsugi, Japan

K. Tanaka
Pharmacology, PET Center, Shonan-Atsugi Hospital, Atsugi, Japan

Introduction

The diagnosis of Alzheimer's disease (AD) is based on the National Institute of Neurological and Communicative Disorders and Stroke-Alzheimer's Disease and Related Disorders Association (NINCDS-ADRDA) criteria [1]. Some non-AD dementias also fulfill the NINCDS-ADRDA criteria, and it is likely that they are included in AD. The criteria have been validated against neuropathological gold standards with diagnostic accuracy ranging from 65 to 96 % [2]. Recently, the National Institute on Aging (NIA)-Alzheimer's Association working group has proposed diagnostic criteria for the spectrum of AD, supported by distinctive and reliable biomarkers of AD which are available through structural MRI, molecular neuroimaging with positron emission tomography (PET), and cerebrospinal fluid analyses [3]. Including the pathologically linked biomarkers of AD in clinical diagnosis could potentially improve diagnostic accuracy, especially at the earliest symptomatic stage.

The AD pathology has been studied in vivo by PET with a selective imaging ligand for amyloid beta (Aβ). The PET tracer is 11C-labeled Pittsburgh compound B

([11C]PIB: *N*-methyl-[11C]2- (4′-methylaminophenyl)-6-hydroxybenzothiazole), which is a derivative of a fluorescent amyloid dye, thioflavin T, that has high affinity and specificity for fibrillar Aβ [4]. The [11C]PIB PET studies in AD patients have consistently demonstrated increased PIB retention in the brain [5, 6]. Furthermore, the retention of PIB measured by PET imaging was directly related to Aβ-containing amyloid plaques in a postmortem study of the AD brain [7]. Recently, we demonstrated that amyloid deposition by [11C]PIB PET allows for an earlier and more specific AD diagnosis [8]. Amyloid PET with [11C]PIB is a reliable biomarker of AD that will facilitate a diagnosis of AD. However, the use of [11C]PIB is limited to centers with an on-site cyclotron because of the short 20-min radioactive half-life of [11C]PIB. The [11C]PIB PET is a serious barrier to increasing the accessibility of this biomarker for routine clinical purposes.

18F-Labeled amyloid radiotracers appear to be the best alternative because the 110-min half-life of 18F allows the centralized production and delivery of compounds. Recently, 18F-labeled ligands derived from stilbene, [18F]florbetaben and [18F]florbetapir, have progressed through clinical trials [9, 10]. PET studies with [18F]florbetapir have demonstrated a high specificity and sensitivity for detecting AD and confirmed the postmortem Aβ distribution [9]. Amyloid PET with [18F]florbetapir has been approved for clinical use by the US Food and Drug Administration and the European Medicines Agency. [18F]Flutemetamol (FMM) and [18F]AZD4695, 18F-labeled amyloid tracers that have a close structural analog to [11C]PIB, have also been developed [11, 12]. In particular, [18F]FMM, which is an analog of thioflavin T, is a fluorinated derivative of the widely studied [11C]PIB and is structurally identical to [11C]PIB apart from the presence of 3′ [18F]fluorine [12]. The studies with [18F]FMM PET have reported that both qualitative visual ratings and cortical standardized uptake value ratios (SUVR) quantification show high sensitivity and specificity for distinguishing AD patients from healthy control (HC) subjects [12, 13].

In the present study, our aim was to identify the Aβ deposition by PET imaging with [18F]FMM across the spectrum of AD and to differentiate patients with AD or mild cognitive impairment (MCI) from normal HC subjects. Furthermore, we compared Aβ deposition between [18F]FMM and [11C]PIB PET imaging.

Materials and methods

Subjects

One hundred sixty-six Japanese participants were recruited from our memory clinic and through a community advertisement. They underwent neurological and neuropsychological assessment and neuroimaging. The apolipoprotein E (apoE) genotype was determined from venous blood samples. Global cognitive status was assessed with the Mini-Mental State Examination (MMSE) [14], and the severity of dementia was rated on the Clinical Dementia Rating (CDR) scale [15]. The CDR sum of boxes (CDR SB) score was a simple sum of the score obtained in each of the six rated domains. A semantic memory measure of immediate and delayed recall of a paragraph from the Wechsler Memory Scale-Revised (WMS-R) Logical Memory II was conducted as a simple episodic memory test [16].

Thirty-six patients with AD were older than 56 years and met the core clinical criteria of the NIA-Alzheimer's Association for probable AD [17]. Sixty-eight patients with MCI were older than 56 years and met the core clinical criteria for MCI proposed by the NIA-Alzheimer's Association [18], including concern about a change in cognition, impairment in one or more cognitive domains, preservation of independence in functional abilities, and no dementia. The MMSE score was greater than or equal to 24, and the global CDR score was at least 0.5 in the memory domain. Sixty-two HC subjects had normal cognitive function and no history of neurological or psychiatric diseases. Of the 62 HC subjects, 41 were 56 years of age or older (older HC), 10 were between 46 and 55 years of age (transitional HC), and 11 were 45 years old or younger (young HC). The normal cognitive status of HC subjects was required to be a MMSE score of 28 or greater and a CDR score of 0. Participants were excluded if they had other systemic or brain diseases, including degenerative, vascular, depressive, medical comorbidities, mixed disease, or traumatic brain injury.

The study was approved by the Ethics Committee of the Mirai Iryo Research Center Inc. (Tokyo, Japan). All subjects or their caregiver provided written informed consent for participation.

Tracer synthesis

[18F]FMM is a radioactive 18F-labeled PET diagnostic imaging agent. The active component of [18F]FMM is 2-[3-[18F]-fluoro-4-(methylamino) phenyl]-6-benzothiazolol. [18F]FMM is a fluorinated derivative of the widely studied [11C]PIB and is a neutral and nonionic analog of thioflavin T [12]. [18F]FMM was synthesized on a FASTlab (GE Healthcare) at our PET center according to good manufacturing practice guidelines (PIC/S GMP Guide Annex 3). The average total FMM chemical content was 0.37±0.19 μg/ml, and the average radiochemical purity was 98.5±1.3 %. [11C]PIB was also produced in our PET center according to standard procedures, as previously described [8].

PET imaging

All 166 subjects underwent an [11C]PIB PET scan on the same day as the cognitive testing and an [18F]FMM scan on the next

day without exception. Both scans were done at our PET center. PET imaging was conducted using a Siemens ECAT ACCEL scanner with an axial field of view of 155 mm, providing 63 contiguous 2.4-mm slices with a 5.6-mm transaxial and a 5.4-mm axial resolution. Images were reconstructed with an iterative reconstruction algorithm, using a Gaussian filter of 3.5-mm full-width at half-maximum. The subject's head was immobilized to minimize motion during the scan.

[11C]PIB was injected intravenously as a bolus with a mean dose of 551.5 ± 39.7 MBq. Dynamic PET scanning in three-dimensional mode was performed for 60 min using a predetermined protocol of 31 frames as follows: 4×15 s, 8×30s, 9×60s, 2×120 s, and 8×300 s. A single dose of [18F]FMM of 197.0 ± 5.9 MBq was injected as a bolus. The image acquisition window of [18F]FMM extended from 85 to 115 min (6×5-min frames). All subjects underwent volumetric T1-weighted MRI (1.5 T Toshiba scanner) for screening and subsequent coregistration with the PET images.

Vital signs and clinical status were checked before and after PET scanning for each subject, and follow-up visits were conducted. Subjects were observed for adverse events and serious adverse events from the first administration of tracer, immediately after the scan, and during the follow-up period.

Image analysis

A region of interest (ROI) analysis was performed on individual PET images. MRI-based correction of PET data was carried out using the PMOD software package (PMOD Technologies Ltd., Adliswil, Switzerland). The ROIs (one slice) were manually drawn on the coregistered MR image along the anterior commissure-posterior commissure (AC-PC) plane in each subject and included the following 20 bilateral cortical regions: lateral temporal cortex (LTC), medial temporal cortex (MTC), frontal cortex (FC), occipital cortex (OC), parietal cortex (PC), sensorimotor cortex (MC), anterior cingulate gyrus (ACG), posterior cingulate gyrus (PCG), precuneus cortex (Pre), and cerebellar cortex. The cerebellar gray matter was used as a reference region.

The retention of [18F]FMM was calculated as the regional to cerebellum SUVR. SUV, defined as the decay-corrected brain radioactivity concentration, were normalized for the injected dose and body weight. The regional FMM SUVR in each cortical region and cortical FMM SUVR for the mean of regional SUVR over nine cortical regions, including LTC, MTC, FC, OC, PC, MC, ACG, PCG, and Pre, were defined. The retention of [11C]PIB was determined by the distribution volume ratio (DVR) with Logan graphical analysis for 35–60 min with cerebellar gray matter as the reference [6] and was additionally calculated as the SUVR. Regional and cortical PIB DVR and PIB SUVR values were calculated in the same regions as the FMM SUVR.

For visual inspection, [18F]FMM PET images were displayed and read using a rainbow color scale. Prior to this assessment, readers were trained with typical positive and negative [18F]FMM images for an AD patient with a typical [11C]PIB-positive scan and an HC subject with an [11C]PIB-negative scan, both of whom were recruited from our studied subjects as previously reported [8] (unpublished data). [18F]FMM images were visually assessed by three readers blinded to clinical diagnosis. The readers used a binary scale to classify each scan as positive or negative for [18F]FMM retention. A "positive scan" had an increased [18F]FMM uptake in any or all cortical regions and was classified as typical positive or focal positive. A "negative scan" showed no FMM uptake in any of the cortical regions. The visual rating was rerun until readers reached consensus for each case. The sensitivity and specificity of visual assessment of the AD and HC scans were calculated, with the baseline clinical diagnosis as the standard of truth (SOT). Interreader agreement was calculated by means of Fleiss' κ coefficient based on the initial reads and the intrareader agreement rate was also evaluated.

Since [11C]PIB PET images were evaluated previously in our [11C]PIB PET study of AD [8], we did not have a specific training for visual assessment. Scans in all subjects were visually read by the same three readers as being positive or negative for [11C]PIB retention, similar to the [18F]FMM visual assessment.

Quantitative threshold between AD and HC

We introduced a complementary threshold procedure and evaluated the SUVR values in discriminating AD patients from HC subjects. The threshold between HC and AD was based on 11 young HC subjects (aged≤45) and 10 transitional HC subjects (aged 46–55) with negative images and 32 AD patients with typical positive images. Readers had complete agreement on these images for typical positive and negative findings, which were the same as for [11C]PIB PET images.

Statistical analysis

Group differences were evaluated with multiple comparisons using Bonferroni post hoc tests to assess the significance. Pearson's correlation analyses were conducted among the FMM SUVR, PIB DVR, and clinical features. Categorical variables were examined with Fisher's exact test. Results were considered significant at $p<0.05$. Data were presented as means ± standard deviations (SD). Statistical analyses were performed with Statcel 3 software (OMS Inc., Tokyo, Japan).

Results

Clinical data and cognitive function

The demographic characteristics of the AD and MCI patients and older HC, transitional HC, and young HC subjects are shown in Table 1. All patients in the AD, MCI, and older HC groups were 56 years of age or older, and the AD group differed slightly in their age and sex distributions from other groups. The transitional HC subjects ranged in age from 46 to 55 (mean 50.8±3.2), while young HC subjects were less than 45 years old (mean 39.5±4.9). They had no cognitive impairment. The 36 patients with AD had a mean MMSE score of 19.4±4.6, a global CDR score of 0.9±0.4, and a CDR SB score of 3.5±2.1, which represented significantly greater cognitive impairment compared with the older HC subjects and the MCI patients. The 68 patients with MCI had a mean MMSE score of 27.4±1.7 and a CDR SB score of 0.6±0.2. For the memory measure of WMS-R Logical Memory II Immediate and Delayed Recall, the mean delayed paragraph recall scores in AD and MCI patients were 0.5±1.1 and 5.2±4.4, respectively, which were significantly lower than that in older HC subjects, despite their having approximately the same level of education. An apoE ε4 allele was present in 58.3 % of AD patients, which was significantly different from older HC subjects (36.5 %).

Safety analysis

No significant effects of tracer administration on vital signs were detected. Adverse events and serious adverse events were not observed after the administration of the tracers, immediately after the scan, and during the follow-up period.

[18F]FMM PET imaging was generally safe and well tolerated by all subjects in this study.

Visual analysis

The axial and sagittal slices of representative typical positive images on [18F]FMM PET in AD and MCI patients and a representative negative image in an older HC subject are shown in Fig. 1. The typical positive image in the AD patient showed extensive [18F]FMM uptake in the frontal, parietal, and lateral temporal cortical regions as well as the cingulate gyrus and precuneus, similar to that in the MCI patient. In contrast, the negative image showed high nonspecific [18F]FMM uptake only in white matter but no increased uptake in any cortical region. PET images revealed the clear difference in cortical [18F]FMM retention between AD and HC subjects. Also, the typical positive and negative images on [18F]FMM PET are compared with those on [11C]PIB in the same patient and are presented in Fig. 2. The typical positive image on [18F]FMM PET showed the loss of the gray-white matter demarcation with high cortical uptake, while that on [11C]PIB PET showed higher uptake in the gray matter than in the white matter. The negative image on [18F]FMM PET had high uptake only in the white matter, which was more pronounced than that on [11C]PIB.

Of 36 AD patients, 35 (97.2 %) had positive scans: 32 of these patients had typical positive scans, and 3 had focal positive scans with increased regional [18F]FMM uptake in the precuneus and/or parietal cortical regions. One AD patient had a negative scan. In contrast, all 11 young and 10 transitional HC subjects had negative scans, while 35 of 41 older HC subjects had negative scans. The remaining six (14.6 %) subjects had positive scans, of whom four had typical positive

Table 1 Demographic characteristics of the AD, MCI, and HC groups

	AD	MCI	Older HC	Transitional HC	Young HC
n	36	68	41	10	11
Female	26 (72.2%)	37 (54.4%)	18 (43.9%)	7 (70%)	7 (63.6%)
Age (years)	76.8±7.5	71.9±7.6	66.9±5.4	50.8±3.2	39.5±4.9
Education (years)	10.3±2.1	12.2±2.3	13.8±2.2	14.4±1.8	14.7±1.8
MMSE	19.4±4.6	27.4±1.7	29.4±0.6	29.8±0.6	29.2±0.9
Global CDR	0.9±0.4	0.5	0	0	0
CDR SB	3.5±2.1	0.6±0.2	0	0	0
Immediate Rec	2.5±2.4*	7.7±4.2*	13.9±3.2	16.9±2.4	17.0±3.4
Delayed Rec	0.5±1.1*	5.2±4.4*	11.6±3.6	15.8±2.5	16.2±3.3
apoE ε4 carrier	21 (58.3%)*	22 (32.3%)	15 (36.5%)	0	2 (18.1%)

Data are presented as means ± SD

AD Alzheimer's disease, *MCI* mild cognitive impairment, *HC* healthy control, *n* number of patients, *MMSE* Mini-Mental State Examination, *CDR* Clinical Dementia Rating, *CDR SB* Clinical Dementia Rating sum of boxes score, *Rec* WMS-R recall scores, *apoE* apolipoprotein E

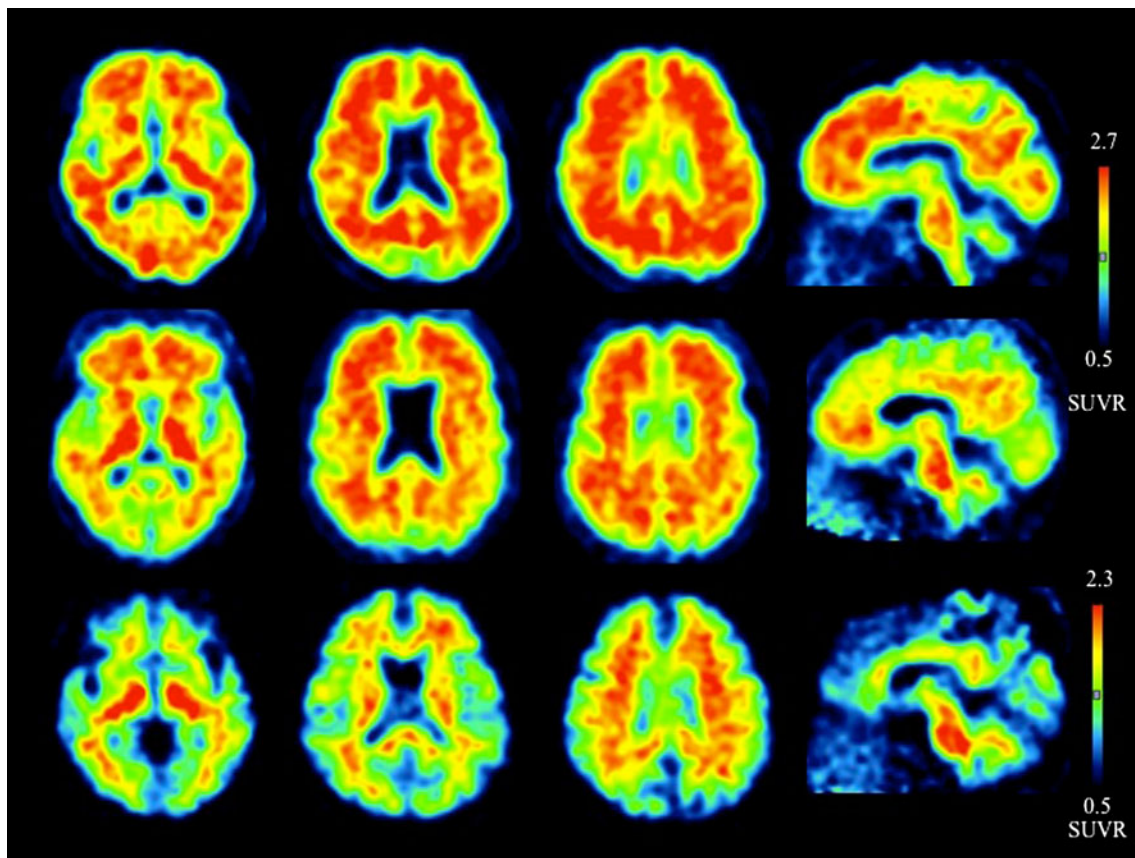*Statistically significant difference by multiple comparisons post hoc tests ($p < 0.05$)

Fig. 1 Representative axial and sagittal [18F]FMM PET images of AD, MCI, and older HC subjects. Typical positive images from AD (*upper*) and MCI (*middle*) patients show extensive [18F]FMM uptake in cortical regions, while negative images from older HC (*lower*) subjects show nonspecific [18F]FMM uptake in white matter

scans, while two had focal positive scans with regional [18F]FMM uptake in the precuneus and/or frontal cortical regions. Based the majority of the results read, [18F]FMM PET scans discriminated AD patients from older HC subjects with a sensitivity of 97.2 % and a specificity of 85.3 %, and young and transitional HC subjects with a specificity of 100 %, which were the same results obtained with [11C]PIB PET scans. Interreader agreement was high, reaching kappa values of 0.81, and the overall intrareader agreement rate was high (93 %). Among 68 patients with MCI, 29 (42.6 %) had positive scans, while 39 had negative scans. Of 29 MCI patients with positive scans, 22 were typical positive and 7 were focal positive, of whom 6 patients had an increased uptake in the precuneus, 4 in the parietal cortical region, and 2 in the frontal cortical region, respectively.

Quantitative analysis

The cortical FMM SUVR values for the AD and MCI patients and older HC subjects are presented in Fig. 3. The mean cortical FMM SUVR in AD patients was 1.76 ± 0.23 ($n = 36$, $p < 0.01$), which was higher than that in the older HC subjects (1.30 ± 0.26, $n = 41$) or the MCI patients (1.42 ± 0.31, $n = 68$).

In contrast, the mean cortical PIB DVR in AD was 1.93 ± 0.37 ($n = 36$, $p < 0.01$), which was higher than in older HC or MCI patients. The cortical SUVR for FMM in AD patients was 37.6 % greater than in older HC subjects, while cortical DVR for PIB in AD was 49.6 % greater.

The mean values of regional FMM SUVR and PIB DVR in nine cortical regions of the AD, MCI, and older HC groups are shown in Table 2. The regional FMM SUVR and PIB DVR values in all eight cortical regions except for MTC were significantly higher in the AD group than in the older HC group. The regional SUVR of the AD group was greater in Pre, PCG, FC, PC, and LTC and less in OC and SMC. The mean FMM SUVR in the precuneus for AD patients was the greatest among cortical regions, compared with that for older HC subjects.

Individual cortical FMM SUVR values in young and transitional HC subjects with negative scans and AD patients with typical positive scans are shown in Fig. 4. The mean cortical SUVR values of young and transitional HC subjects were 1.18 ± 0.09 ($n = 11$, $p < 0.01$) and 1.21 ± 0.13 ($n = 10$, $p < 0.01$), significantly different from those of AD patients (1.85 ± 0.22, $n = 32$). The maximum cortical FMM SUVR in young HC subjects was 1.35. In AD patients, the minimum cortical SUVR

Fig. 2 Representative [18F]FMM and [11C]PIB PET images of the same patient with typical positive (*upper*) and negative scans (*lower*). The typical positive image on [18F]FMM PET shows the cortical uptake with a loss of the gray-white matter demarcation, while the [11C]PIB image shows distinctly high uptake in gray matter

FMM SUVR   PIB DVR
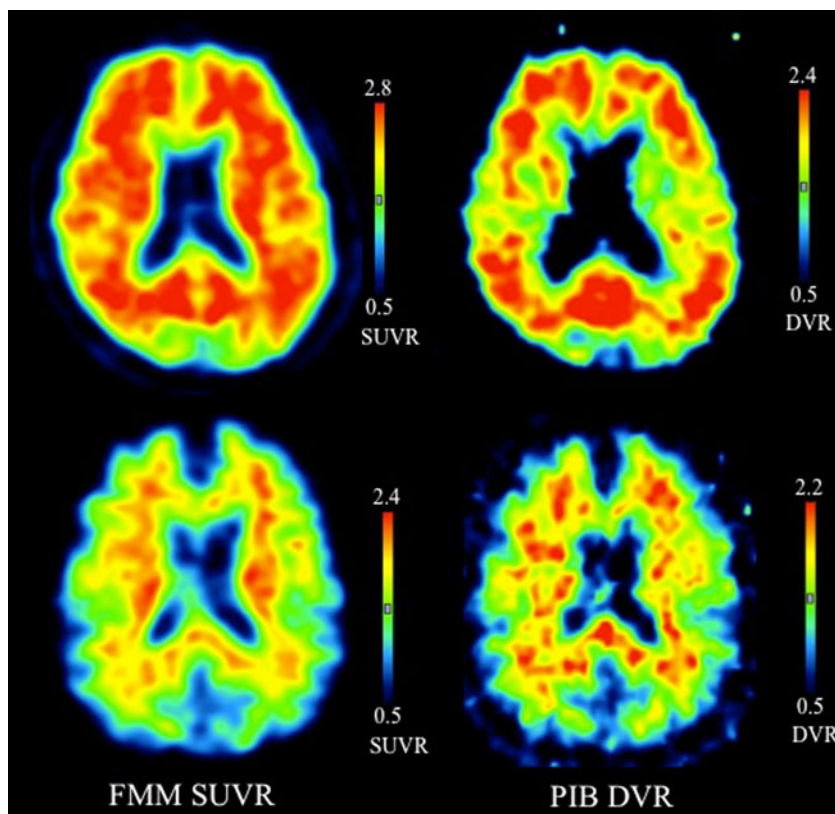
was 1.50 regardless of apoE ε4. A cortical FMM SUVR of ≤1.35 was used as the FMM-negative threshold, while a cortical SUVR value of ≥1.50 was used as the FMM-positive threshold in our clinical setting. A cortical SUVR between these threshold values was interpreted as intermediate. For each cortical region, a regional SUVR threshold was different, and the minimum value in each region of these AD patients was

used as the FMM-positive threshold. Of all 36 AD patients, 32 (88.8 %) had high cortical SUVR above the FMM-positive threshold, while 2 were FMM negative and 2 had intermediate SUVR. In contrast, 34 (82.9 %) of 41 older HC subjects were FMM negative and 5 were FMM positive. The remaining two older HC subjects were intermediate. Among 68 MCI patients, 23 (33.8 %) had high SUVR above the FMM-positive

Fig. 3 Individual and mean cortical FMM SUVR values in older HC subjects and AD and MCI patients. Data are presented as mean ± SD. *Statistically significant difference by multiple comparisons post hoc tests ($p < 0.01$)
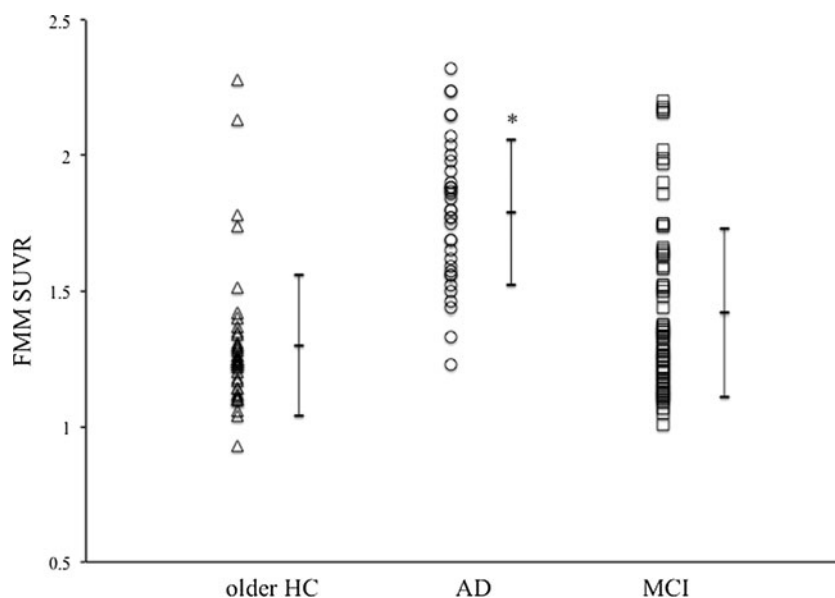
Table 2 Regional FMM SUVR and PIB DVR values in cortical regions of OHC, AD, and MCI patients and the relationship between FMM SUVR and PIB DVR

Region	FMM SUVR			PIB DVR			r
	OHC	AD	MCI	OHC	AD	MCI	
MTC	1.21±0.11	1.23±0.16	1.20±0.15	1.14±0.18	1.24±0.20	1.16±0.15	0.69
LTC	1.22±0.26	1.77±0.28*	1.36±0.33	1.22±0.30	1.93±0.40*	1.35±0.37	0.93
ACG	1.38±0.34	2.10±0.38*	1.49±0.45	1.35±0.47	2.29±0.48*	1.50±0.53	0.94
FC	1.34±0.33	2.08±0.33*	1.48±0.43	1.30±0.41	2.15±0.40*	1.43±0.42	0.90
OC	1.35±0.19	1.59±0.23*	1.39±0.23	1.30±0.17	1.60±0.29*	1.39±0.22	0.85
PCG	1.40±0.36	2.09±0.36*	1.48±0.47	1.41±0.42	2.22±0.45*	1.51±0.45	0.92
Pre	1.36±0.42	2.16±0.36*	1.50±0.50	1.40±0.51	2.44±0.53*	1.53±0.53	0.95
PC	1.18±0.32	1.79±0.38*	1.33±0.41	1.23±0.38	2.04±0.43*	1.35±0.41	0.92
SMC	1.24±0.24	1.60±0.32*	1.33±0.28	1.21±0.27	1.64±0.36*	1.31±0.25	0.88

OHC older healthy control, *AD* Alzheimer's disease, *MCI* mild cognitive impairment, *MTC* medial temporal cortex, *LTC* lateral temporal cortex, *ACG* anterior cingulate gyrus, *FC* frontal cortex, *OC* occipital cortex, *PCG* posterior cingulate gyrus, *Pre* precuneus, *PC* parietal cortex, *SMC* sensorimotor cortex, *r* Pearson's coefficient for FMM SUVR and PIB DVR

*Statistically significant difference by multiple comparisons post hoc tests ($p<0.05$)

threshold, while 40 were FMM negative. Five MCI patients had intermediate cortical SUVR.

Quantitative analysis and visual assessment

The relationship between individual cortical FMM SUVR and visual assessment in the older HC subjects and AD and MCI patients is shown in Fig. 5. All older HC subjects and AD and MCI patients who had typical positive scans were FMM positive for the cortical SUVR. Among 12 patients with focal positive scans, 1 HC subject and 1 MCI patient were FMM positive. The remaining ten patients had high regional SUVR

above the FMM-positive threshold in focal cortical regions, even though cortical SUVR were FMM negative or intermediate. In contrast, 34 of 35 older HC subjects and 1 AD and 39 MCI patients with negative scans were FMM negative. One HC subject and one MCI patient had intermediate cortical SUVR but no high regional SUVR above the FMM-positive threshold in any cortical region.

Comparison between FMM SUVR and PIB DVR

The relationships between individual cortical FMM SUVR and PIB DVR values for 36 AD and 68 MCI patients and 41

Fig. 4 Individual cortical FMM SUVR values in young HC (≤45 years of age) and transitional HC subjects (46–55 years of age) and AD patients with apoE ε4 (ε4+) and without apoE ε4 (ε4−). The *upper dotted line* indicates the threshold of FMM-positive SUVR, while the *lower line* indicates FMM-negative SUVR
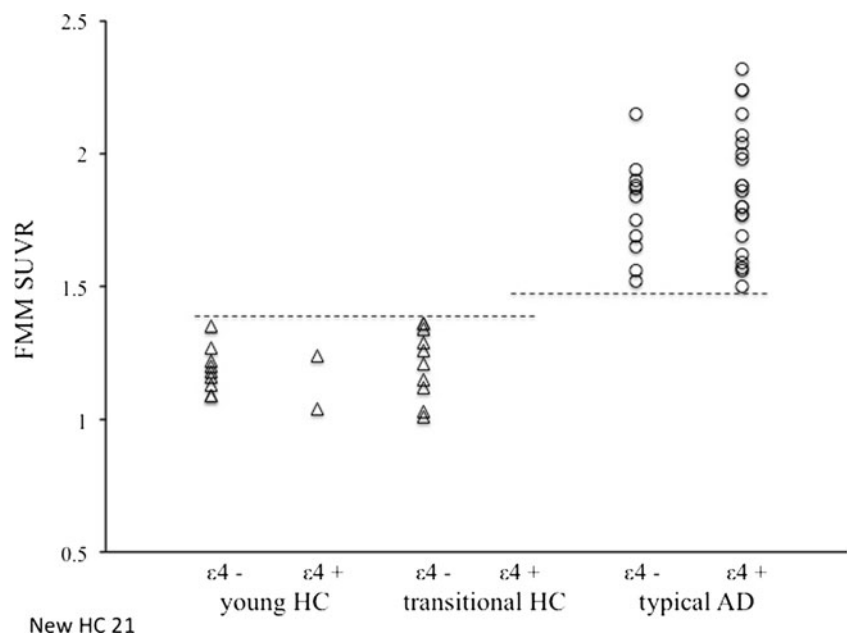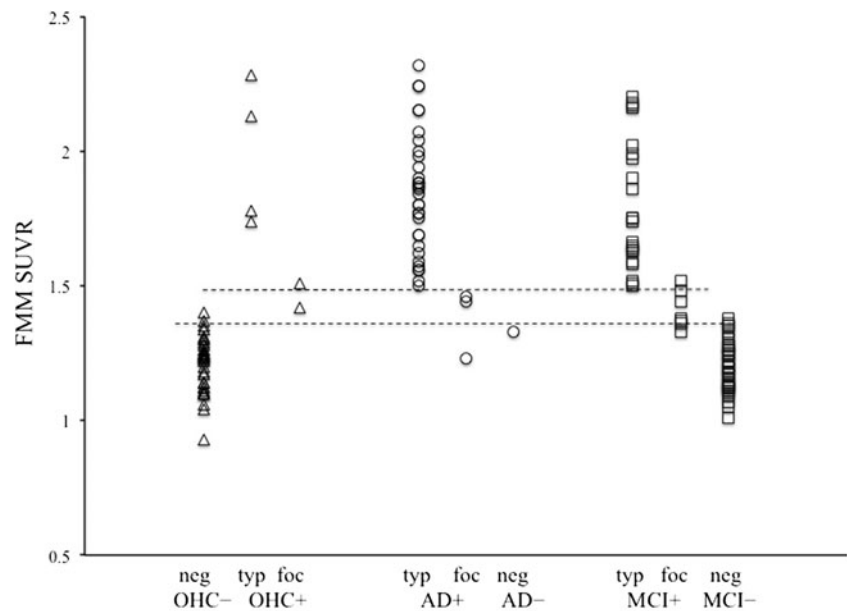
Fig. 5 Individual cortical FMM SUVR values in older HC subjects (OHC) and AD and MCI patients with typical positive (typ), focal positive (foc), and negative (neg) scans. The *upper dotted line* indicates the threshold for FMM-positive SUVR, while the *lower line* indicates FMM-negative SUVR. +: positive scan, −: negative scan

older HC subjects are shown in Fig. 6. The cortical FMM SUVR was highly correlated with PIB DVR in the same patients ($r=0.94$, $p<0.001$). Furthermore, all 58 patients with high SUVR above the FMM-positive threshold exceeded the threshold of positive PIB DVR, when the minimum PIB DVR in AD patients was 1.56 and was defined as PIB positive. The cortical FMM SUVR was also highly correlated with PIB SUVR in the same patients ($r=0.96$, $p<0.001$), similar to PIB DVR.

The relationship between regional FMM SUVR and PIB DVR values in nine cortical regions of AD and MCI patients and older HC subjects are shown in Table 2. For each of nine cortical regions, regional FMM SUVR values were significantly correlated with the corresponding regional PIB DVR (Pearson's coefficient ranged from 0.69 for the MTC to 0.95 for the Pre, $p<0.001$).

FMM SUVR, age, apoE genotype, and cognitive function

There was no significant difference in the mean cortical FMM SUVR between apoE $\varepsilon4$ carriers and noncarriers in each group (Fig. 7). However, all 21 AD patients with apoE $\varepsilon4$ had a high SUVR, while all 3 AD patients with a low SUVR were apoE $\varepsilon4$ noncarriers. In addition, four of five older HC patients with high SUVR were apoE $\varepsilon4$ carriers.

There was a weak, but significant relationship between cortical FMM SUVR and age in all groups ($r=0.33$, $n=145$, $p<0.001$). In contrast, cortical FMM SUVR was not related to age in the AD or MCI groups, but it was related in the older HC group ($r=0.41$, $n=41$, $p<0.01$).

Cortical FMM SUVR was negatively correlated with MMSE scores ($r=-0.51$, $n=145$, $p<0.05$) and positively

with CDR SB scores ($r=0.49$, $n=145$, $p<0.05$) when all groups were analyzed together. However, there was no significant correlation between cortical FMM SUVR and MMSE score in older HC subjects ($r=0.21$) or in MCI ($r=-0.23$) or AD patients ($r=-0.18$).

Discussion

We demonstrated that [^{18}F]FMM PET scans discriminated AD patients from older HC subjects with a sensitivity of 97.2 % and specificity of 85.3 % and from young and transitional HC subjects with a specificity of 100 %. A phase II clinical study of [^{18}F]FMM amyloid imaging has reported that the sensitivity and specificity of the visual PET scan assessment in AD patients and elderly HC subjects is 96 and 93 %, respectively [13]. These findings are consistent with the visual assessments of amyloid PET imaging with other ^{18}F-labeled tracers in that the sensitivity ranges from 80 to 96 % and specificity from 90.5 to 100 % for distinguishing AD patients [9, 10, 13]. In addition, our results were confirmed by a recent autopsy study showing that the visual interpretation of [^{18}F]FMM PET imaging correlated with the NIA-Reagan neuropathological criteria for the probability of AD [19]. We suggest that amyloid PET imaging with [^{18}F]FMM discriminates AD patients from older HC subjects with sufficient sensitivity and specificity.

Some studies with ^{18}F-labeled amyloid PET imaging have reported that the nonspecific binding of ^{18}F-labeled tracers to white matter is high compared with [^{11}C]PIB [9, 10, 13]. The accurate interpretation of ^{18}F-labeled amyloid images might require a training program. In the present study, [^{18}F]FMM

Fig. 6 Scatter plot of the relationship between cortical FMM SUVR and PIB DVR values in older HC subjects (*triangles*), AD (*circles*), and MCI patients (*squares*). Cortical FMM SUVR is significantly correlated with PIB DVR in individual subjects (**a**). The *vertical dotted line* indicates the threshold of FMM-positive SUVR, while the *horizontal line* indicates the threshold of PIB-positive DVR (**b**). All individuals with an FMM-positive SUVR have a PIB DVR above the threshold
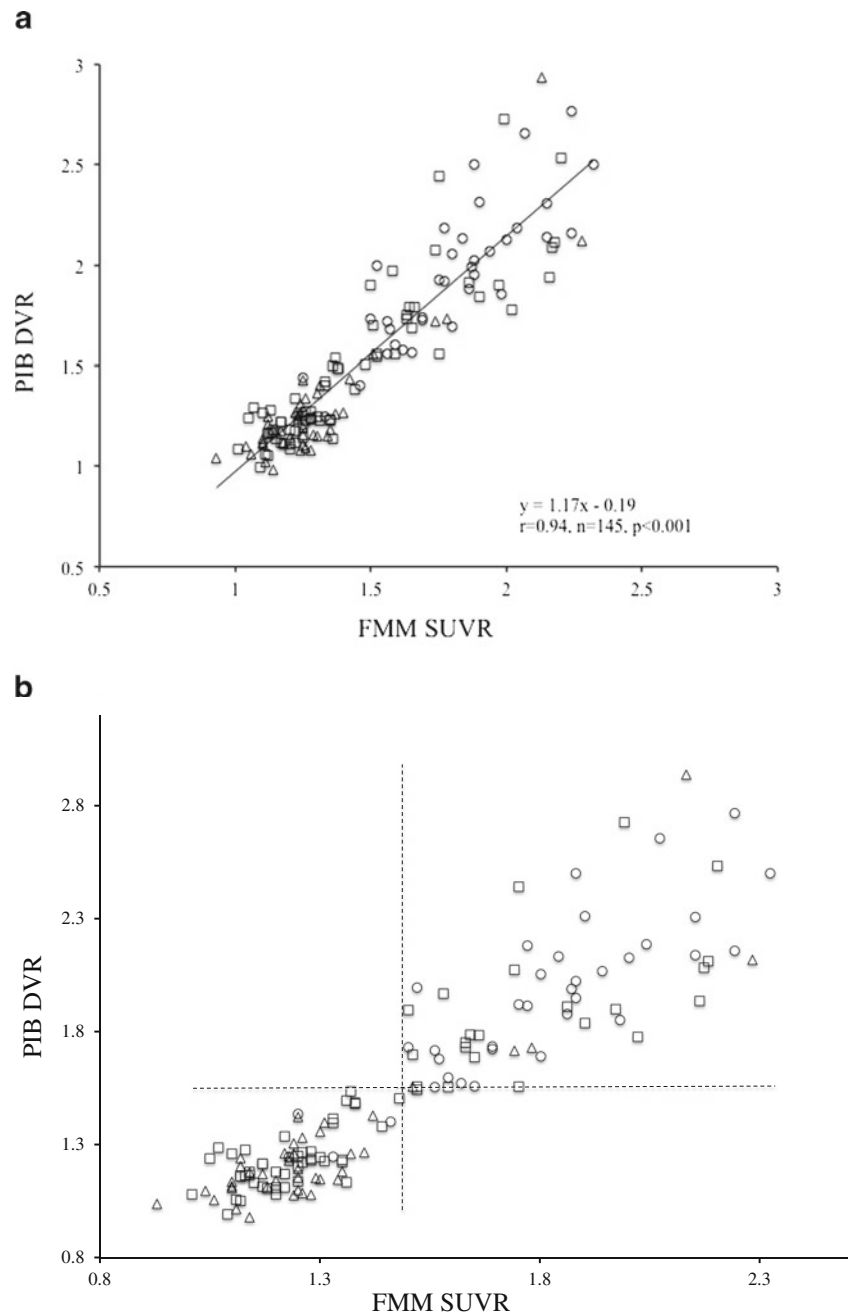

uptake in PET images was increased in white matter, although the [18F]FMM binding to white matter varied between subjects. In addition, the positive image in [18F]FMM PET revealed no gray-white matter demarcation as the predominant evidence of cortical Aβ deposition, while that on [11C]PIB PET indicated high Aβ retention in gray matter with excess retention in white matter. A loss of the distinct grey-white matter contrast with cortical [18F]FMM uptake is important to the visual assessment of an [18F]FMM scan. Therefore, the higher nonspecific FMM binding to white matter could not lead to any misclassification of the scans by trained visual readers with experience in the orientation and interpretation of amyloid images.

Establishing standards for image acquisition and the thresholds between high and low cortical FMM SUVR are needed to facilitate the comparison of data among different subjects across the continuum of AD. We found that 97.2 % of 36 AD patients had high cortical and/or regional SUVR above the FMM-positive threshold, while 85.3 % of the 41 older HC subjects were FMM negative. In contrast, 42.6 % of the 68 MCI patients had high cortical SUVR above the FMM-positive threshold or high regional SUVR in some cortical

Fig. 7 Individual and mean cortical FMM SUVR values in apoE ε4 carriers (ε4+) and noncarriers (ε4−) with older HC, AD, and MCI patients. There is no significant difference in mean FMM SUVR between apoE ε4 carriers and noncarriers. All apoE ε4 carriers with AD have a high FMM SUVR. Data are presented as mean ± SD
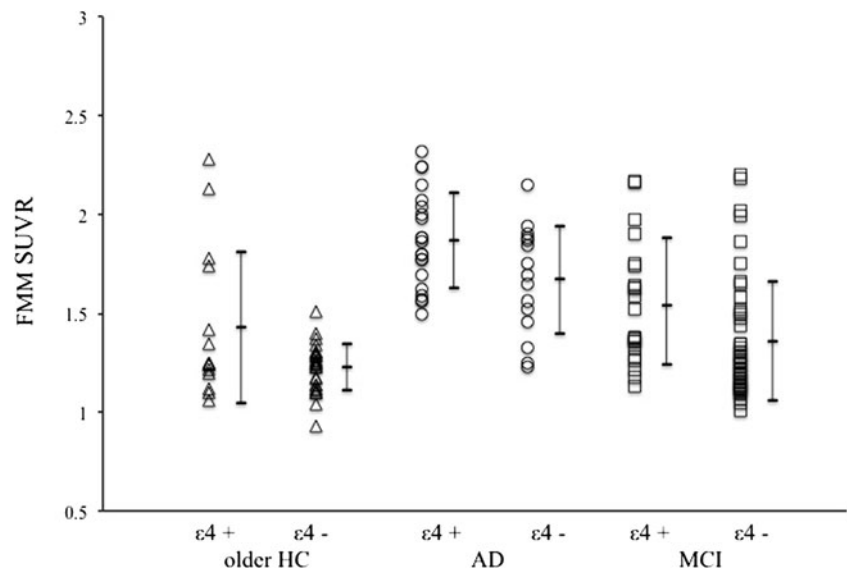
regions. These findings were completely identical to those with visual assessment of [18F]FMM PET images. Thus, the threshold of cortical and regional FMM SUVR was successfully defined in our clinical setting based on the AD patients with typical positive scans and young HC subjects, being well known as low-risk individuals. We suggest that the discrimination between amyloid-positive and amyloid-negative subjects on [18F]FMM PET could be achieved by both visual image interpretation and a simple semiquantitative measure. It is important for future routine clinical use that the accurate quantification of [18F]FMM PET is possible in an automated, objective, and independent manner.

We demonstrated that 97.2 % of 36 AD patients had positive scans, while only 1 patient had a negative scan on both [18F]FMM and [11C]PIB PET. The neuropathological study of [18F]FMM PET has demonstrated that positive [18F]FMM images correlate highly with moderate or frequent Aβ neuritic plaques in the postmortem brain [19]. Therefore, a negative finding on [18F]FMM images for AD patients may be attributable to incorrect clinical diagnoses or impossibly be detected with amyloid PET because of insufficient Aβ neuritic plaques. Severe cortical atrophy will also make image interpretation more difficult. On the other hand, 14.6 % of 41 older HC subjects had positive scans, which was identical to the [11C]PIB PET scans of the same subjects. Our previous [11C]PIB PET study has demonstrated that 18 % of 91 cognitively normal older adults have increased amyloid deposition in cortical regions [8]. In the [18F]florbetaben PET study, 10 % of healthy controls have been reported to be Aβ positive [10]. These findings are consistent with an autopsy study reporting that 20–34 % of healthy elderly adults aged over 75 years have AD neuropathology [20]. The Aβ deposition in the brain is an early event and likely to occur before cognitive impairment. The [18F]FMM PET can identify preclinical AD as an Aβ

biomarker, similar to [11C]PIB PET. The present study also found that 42.6 % of 68 MCI patients had positive scans for [18F]FMM PET. This proportion is similar to the finding reported in amyloid PET imaging studies with 18F-labeled tracers in addition to [11C]PIB [21]. In addition, we have recently demonstrated, using [11C]PIB PET imaging, that 56.8 % of 51 MCI patients with Aβ deposition converted to AD over 2 years, compared with 5.8 % of 17 MCI patients without Aβ deposition [22]. Therefore, an [18F]FMM-positive scan can identify MCI with a high risk of converting to AD, while an [18F]FMM-negative scan has a very high negative predictive value excluding progression to AD.

Comparisons of the [11C]PIB and 18F-labeled amyloid tracers have been studied for amyloid PET imaging in dementia [23, 24]. The present study directly compared [18F]FMM and [11C]PIB images in the same subjects. The cortical FMM SUVR in AD patients was 37.6 % greater than in older HC subjects, while cortical PIB DVR in AD was 49.6 % greater. The degree of Aβ retention was slightly lower for [18F]FMM although the cortical distribution on [18F]FMM PET images was identical to that for [11C]PIB. In contrast, the cortical FMM SUVR was highly correlated with PIB DVR, and all patients with FMM-positive SUVR exceeded the threshold of PIB-positive DVR. These findings indicate that quantitative measurement of [18F]FMM PET images, in addition to visual assessment, is consistent with that of [11C]PIB PET. [18F]FMM PET can reliably detect Aβ deposition in the brain and is useful in the early and differential diagnosis of AD, similar to [11C]PIB PET.

We have demonstrated that [18F]FMM PET provides images that appear similar to [11C]PIB PET images without the limitation of the short 11C radioactive decay half-life although the present study is a single-center evaluation at our institute, different from that in the multicenter clinical trial studies. The

decay half-life of ^{18}F can make centralized production with distribution to multiple PET sites possible, thereby improving access to Aβ imaging. It is highly likely that the [^{18}F]FMM compound will replace [^{11}C]PIB in general clinical practice. [^{18}F]FMM PET could become a routine clinical procedure as a reliable biomarker of Aβ deposition. Our ongoing longitudinal study will determine the potential value of [^{18}F]FMM PET in prodromal and even preclinical AD. Furthermore, it is likely to play a critical role in the development of anti-amyloid therapies by improving subject selection during early phases of the disease and monitoring treatment response.

References

1. McKhann G, Drachman DA, Folstein M, Katzman R, Price D, Stadlan EM. Clinical diagnosis of Alzheimer's disease: report of the NINCDS-ADRDA Work Group under the auspices of Department of Health and Human Services Task Force on Alzheimer's Disease. Neurology 1984;34:939–44.
2. Kazee AM, Eskin TA, Lapham LW, Gabriel KR, McDaniel KD, Hamill RW. Clinicopathologic correlates in Alzheimer disease: assessment of clinical and pathologic diagnostic criteria. Alzheimer Dis Assoc Disord 1993;7:152–64.
3. Jack Jr CR, Albert MS, Knopman DS, McKhann GM, Sperling RA, Carrillo MC, et al. Introduction to the recommendations from the National Institute on Aging-Alzheimer's Association workgroups on diagnostic guidelines for Alzheimer's disease. Alzheimers Dement 2011;7:257–62.
4. Mathis CA, Wang Y, Holt DP, Huang GF, Debnath ML, Klunk WE. Synthesis and evaluation of 11C-labeled 6-substituted 2-arylbenzothiazoles as amyloid imaging agents. J Med Chem 2003;46:2740–54.
5. Klunk WE, Engler H, Nordberg A, Wang Y, Blomqvist G, Holt DP, et al. Imaging brain amyloid in Alzheimer' disease with Pittsburgh Compound-B. Ann Neurol 2004;55:306–19.
6. Price JC, Klunk WE, Lopresti BJ, Lu X, Hoge JA, Ziolko SK, et al. Kinetic modeling of amyloid binding in human using PET imaging and Pittsburgh Compound-B. J Cereb Blood Flow Metab 2005;25: 1528–47.
7. Ikonomovic MD, Klunk WE, Abrahamson EE, Mathis CA, Price JC, Tsopelas ND, et al. Post-mortem correlates of in vivo PiB-PET amyloid imaging in a typical case of Alzheimer's disease. Brain 2008;131:1630–45.
8. Hatashita S, Yamasaki H. Clinically different stages of Alzheimer's disease associated by amyloid deposition with [11C]-PIB PET imaging. J Alzheimers Dis 2010;21:995–1003.
9. Clark CM, Schneider JA, Bedell BJ, Beach TG, Bilker WB, Mintun MA, et al. Use of florbetapir-PET for imaging beta-amyloid pathology. JAMA 2011;305:275–83.
10. Brthel H, Gertz HJ, Dresel S, Peters O, Bartenstein P, Buerger K, et al. Cerebral amyloid-β PET with florbetaben (18F) in patients with Alzheimer's disease and healthy controls: a multicentre phase 2 diagnostic study. Lancet Neurol 2011;10:424–35.
11. Cselenyi Z, Jönhagen ME, Forsberg A, Halldin C, Julin P, Schou M, et al. Clinical validation of 18F-AZD4694, an amyloid-β-specific PET radioligand. J Nucl Med 2012;53:415–24.
12. Neilssen N, Van Laere K, Thurfiell L, Owenius R, Vandenbulcke M, Koole M, et al. Phase 1 study of the Pittsburgh compound B derivative 18F-flutemetamol in healthy volunteers and patients with probable Alzheimer disease. J Nucl Med 2009;50:1251–9.
13. Vandenberghe R, Van Laere K, Ivanoiu A, Salmon E, Bastin C, Triau E, et al. 18F-flutemetamol amyloid imaging in Alzheimer disease and mild cognitive impairment A phase 2 trial. Ann Neurol 2010;68:319–29.
14. Folstein MF, Folstein SE, McHugh PR. "Mini-mental state". A practical method for grading the cognitive state of patients for the clinician. J Psychiatr Res 1975;12:189–98.
15. Morris JC. The Clinical Dementia Rating (CDR): current version and scoring rules. Neurology 1993;43:2412–4.
16. Wechsler DA. Wechsler memory scale-revised. New York: Psychological Corporation; 1987.
17. McKhann GM, Knopman DS, Chertkow H, Hyman BT, Jack Jr CR, Kawas CH, et al. The diagnosis of dementia due to Alzheimer's disease: recommendations from the National Institute on Aging-Alzheimer's Association workgroups on diagnostic guidelines for Alzheimer's Association. Alzheimers Dement 2011;7:263–9.
18. Albert MS, DeKosky ST, Diskson D, Dubois B, Feldman HH, Fox NC, et al. The diagnosis of mild cognitive impairment due to Alzheimer's disease: recommendations from the National Institute on Aging-Alzheimer's Association workgroups on diagnostic guidelines for Alzheimer's disease. Alzheimers Dement 2011;7:270–9.
19. Smith A, Buckley C, Sherwin P, Heurling K, Ikonomovic M, Mathis C, et al. Evaluation of the histopathology burden underlying [18F]flutemetamol PET imaging (abstract). Human Amyloid Imaging 2013;7:32.
20. Bennett DA, Schneider JA, Arvanitakis Z, Kelly JF, Aggarwal NT, Shah RC, et al. Neuropathology of older persons without cognitive impairment from two community-based studies. Neurology 2006;66: 1837–44.
21. Fleisher AS, Chen K, Liu X, Roontiva A, Thiyyagura P, Ayutyanont N, et al. Using positron emission tomography and florbetapir F 18 to image cortical amyloid in patients with mild cognitive impairment or dementia due to Alzheimer disease. Arch Neurol 2011;68(11):1404–11.
22. Hatashita S, Yamasaki H. Diagnosed mild cognitive impairment due to Alzheimer's disease with PET biomarkers of beta amyloid and neuronal dysfunction. PLoS One 2013;8(6):e66877. doi:10.1371/journal.pone.0066877.
23. Villemagne VL, Mulligan RS, Pejoska S, Ong K, Jones G, O'Keefe G, et al. Comparison of 11C-PiB and 18F-florbetaben for Aβ imaging in ageing and Alzheimer's disease. Eur J Nucl Med Mol Imaging 2012;39:983–9.
24. Rowe CC, Pejoska S, Mulligan RS, Jones G, Chan JG, Svensson S, et al. Head-to-head comparison of 11C-PiB and 18F-AZD4694 (NAV4694) for β-amyloid imaging in aging and dementia. J Nucl Med 2013;54:880–6.